Supporting Online Material for

Whole-Genome Shotgun Sequencing of Mitochondria from Ancient Hair Shafts

M. Thomas P. Gilbert, Lynn P. Tomsho, Snjezana Rendulic, Michael Packard, Daniela I. Drautz, Andrei Sher, Alexei Tikhonov, Love Dalén, Tatyana Kuznetsova, Pavel Kosintsev, Paula F. Campos, Thomas Higham, Matthew J. Collins, Andrew S. Wilson, Fyodor Shidlovskiy, Bernard Buigues, Per G. P. Ericson, Mietje Germonpré, Anders Götherström, Paola Iacumin, Vladimir Nikolaev, Malgosia Nowak-Kemp, Eske Willerslev, James R. Knight, Gerard P. Irzyk, Clotilde S. Perbost, Karin M. Fredrikson, Timothy T. Harkins, Sharon Sheridan, Webb Miller,* Stephan C. Schuster*

*To whom correspondence should be addressed.

E-mail: webb@bx.psu.edu (W.M.); scs@bx.psu.edu (S.C.S.)

Published 28 September, *Science* **317**, 1927 (2007)
DOI: 10.1126/science.1146971

This PDF file includes:

Whole-Genome Shotgun Sequencing of Mitochondria from Ancient Hair Shafts

Author contributions

M. Thomas P. Gilbert, Webb Miller and Stephan C. Schuster designed research, carried out data analysis and wrote manuscript; M. Thomas P. Gilbert, Paula F. Campos and Stephan C. Schuster extracted DNA; Webb Miller performed computational analysis and assemblies; Stephan C. Schuster analyzed sequencing-by-synthesis data; Sequencing-by-synthesis and library construction was done by Lynn P. Tomsho and Michael Packard; PCR-resequencing primers (where novel) were designed by M. Thomas P. Gilbert; Snjezana Rendulic and Daniela I. Drautz performed PCR-resequencing at Penn State; Andrei Sher provided the geographic coordinates of the samples and designed the map; Matthew Collins contributed thermal age calculations; computational support for sequencing-by-synthesis was performed by James R. Knight, Gerard P. Irzyk, Clotilde S. Perbost, Karin M. Fredrikson, Timothy T. Harkins, Sharon Sheridan; Andrei Sher, Alexei Tikhonov, Bernard Buigues, Love Dalén, Tatyana Kuznetsova, Pavel Kosintsev, Per G. P. Ericson, Mietje Germonpré, Anders Götherström, Paola Iacumin, Vladimir Nikolaev, Malgosia Nowak-Kemp, Fyodor Shidlovskiy, Eske Willerslev collected, sampled or provided mammoth hair specimens from Siberia and laboratory facilities; Thomas Higham performed C^{14} dating; Andrew S. Wilson performed microscopic analyses on mammoth hair samples.

Supporting Online Material

DNA Sequences submitted to Genbank:

Specimen M1, EU153444; specimen M13, EU153445; specimen M18, EU153447; specimen M2, EU153449; specimen M22, EU153452; specimen M26, EU153454; specimen M3, EU153455; specimen M4, EU153456; specimen M5, EU153457; specimen M8, EU153458, specimen Poinar, EU155210.

Whole-genome shotgun approaches to aDNA

The whole-genome shotgun approach to aDNA does not, as originally applied, target specific genomic markers (however see *S1,S2*), but instead generates sequences in amounts proportional to the molecules' frequencies in the DNA pool. For example, within the mammoth data of Poinar *et al.* (*S3*) the authors observed a ratio of 1:650 mtDNA:nuDNA sequences. Therefore, although the method does not specifically target mtDNA, this ratio in combination with the massive numbers of individual sequences generated in a single sequencing run (>400,000 sequences) allows for the generation of a multiple-fold coverage of this ~16,770-bp circular genome. Thus, Poinar *et al.* (*S3*) generated single-fold coverage of the mammoth mitochondrial genome, while a later study incorporating data from further sequencing reactions on the same DNA extracts increased this to 7.7-fold (*S4*). This enabled the assessment of DNA damage and sequencing error through redundancy, because, in contrast to traditional PCR techniques, the SBS approach does not amplify from a template mixture from a pool of DNA molecules, but rather from a single molecule, confined in a lipid micro-reactor (*S4,S5*).

Although the results of this initial test can be viewed as uneconomical for studies aimed solely at the recovery of mtDNA, methods to increase the fraction of mtDNA in extracts would permit complete mitochondrial genomes to be rapidly and relatively economically generated from ancient samples. We therefore considered alternate sources of DNA that were readily available, less susceptible than bone to DNA damage, and with a higher content of mtDNA. While the exact mtDNA:nuDNA ratios are not known for the different tissues, some cell types, specifically those with high energetic demands, contain elevated levels of mitochondria, and thus mtDNA. In mammals for example, it has been demonstrated that highly metabolically active cells such as muscle and certain neurological tissues contain vastly increased numbers of mitochondria per cell (*S6*). Unfortunately however, except in rare cases such as occasional naturally frozen specimens, e.g. the specimen analyzed by Rogaev *et al.* (*S7*), such tissues are normally absent or inadequately preserved in ancient samples. In contrast, hair is a more commonly found material, and offers a number of benefits as described in the main text. Therefore hair was chosen as the source material for this study.

DNA extraction

Between 0.2 and 5.2 grams of mammoth coat hair shafts were extracted per individual. For full sample details see Supplemental Table 1. It has previously been demonstrated that hair shafts can be readily decontaminated from external sources of contamination, presumably due to their highly keratinized structure and relative lack of porosity in comparison to more conventional sources of aDNA such as bone and tooth (*S8*,*S9*). As hair roots are however less keratinized than hair shafts they are likely more

porous to contaminant uptake. Therefore, we specifically excised any observable roots from the samples prior to DNA extraction. Subsequently the hair shafts were manually washed in 0.1x concentration commercial bleach solution (≈0.5% final NaClO concentration) to remove any mud, debris or contaminant DNA that was on the outside of the hair shaft, then rinsed several (2-6 times, hair volume dependent) in DNA-free H_2O until we were satisfied that all traces of the bleach had been removed. Digestion of the hair shafts was performed overnight at 55°C with rotation, using between 10 and 40ml of the following digestion buffer: 10mM Tris-HCl (pH 8.0), 10mM $NaCl_2$, 2% w/v Sodium Dodecyl Sulfate (SDS), 5mM $CaCl_2$, 2.5mM Ethylene-Diamine-Tetra-Acetic acid (EDTA), (pH 8.0), 40mM Dithiothreitol (DTT; Cleland's reagent) and 10% proteinase K solution (>600 mAU/ml, Qiagen). In several cases where large amounts of hair were digested, after 24 hours digestion was still incomplete. In these cases additional proteinase K and DTT were added to the digestion buffer (10% volume) and digestion was allowed to proceed for a further 24 hours at 55°C. Post digestion DNA was purified twice with phenol and once with chloroform following standard protocols. The aqueous, DNA-containing solution was predominantly concentrated to 200µl using Amicon Ultra-15 Centrifugal Filter Units with a 10kD filter (Millipore).

Supplemental Table 1: Full specimen details

Mammoth	Source Museum	Collection number	Region of Origin	Address	Longitude	Latitude	^{14}C Reference	^{14}C YBP (where determined)	Notes (preservation etc)	Collected by	Collection Year	Contributor
M1	Khatanga Ice Cave - CERPOLEX /Mammuthus		unknown	unknown	unknown	unknown		n.d.		CERPOLEX /Mammuthus	unknown	B Buiges
M2 (Jarkov)	Khatanga Ice Cave - CERPOLEX /Mammuthus	2001/XXXA	Taimyr Peninsula	Bolshaya Balakhnya River	105.4	73.32	Reference (S10)	20380±140	Partial skeleton with soft tissues	CERPOLEX /Mammuthus	1997-1999	B Buiges
M3 (Fishhook)	Khatanga Ice Cave - CERPOLEX /Mammuthus		Taimyr Peninsula	Upper Taimyra River Estuary	99.35.28	74.08.48	Reference (S11)	20620±70	Partial skeleton with soft tissues	CERPOLEX /Mammuthus	1990-2001	B Buiges
M4	Palaeoart.com		unknown	unknown	unknown	unknown	OxA-17098	18545±70		Palaeoart.com	unknown	Palaeoart.com
M5	Palaeoart.com		unknown	unknown	unknown	unknown		n.d.		Palaeoart.com	unknown	Palaeoart.com
M8 (Dima)	Zoological Instutite, Russian Academy of Sciences		Magadan Region	Susuman District, Berelyokh River Basin, Kirgilyakh Creek	147.93	62.67	OxA-17102	46900±700	Baby mammoth mummy	A Logachev	1977	A Tikhonov
M13 (Adams)	Universita Degli Studi Di Parma, Italy		North-East Siberia, Lena Delta	Bykovskiy Peninsula, Mamontovy Khayata	127.5	72.5	Reference (S12)	35800±1200	Complete mammoth skeleton with soft tissies	M Adams	1799/1806	P Iacumin

M18	Institute of Animal and Plant Ecology RAS, Ekaterinburg	KOS-W-1	West Siberia, North, Gydan Peninsula	Taimyr Autonomous Area, Gydan Peninsula, Leskino village vicinity, Mongocha-Yakha River Basin	79.35	72.09	OxA-17116	17125±70	Complete mammoth skeleton with soft tissies	PA Kosintsev	2002	PA Kosintsev
M22	Lena Delta Reserve	LDR-P74	N-E Siberia, Novosibirsk Islands	Bol'shoy Lyakhovsky Islands, Bol'shoy Eterikan River	142.67	73.64	OxA-17111	50200±900		V Dormidontov	2000	T Kuznetsova
M-26	Ice Age Museum, Moscow	F-0308	N-E Siberia, Indigirka R.	Tirekhtyakh River mouth	147.06	68.6	OxA-17114	24740±110	Found together with skull and tusks in soft tissues	F Shidlovskiy	2003	A Sher

Note: Details provided to accuracy level as could be determined from original sources

DNA sequence analysis using the Sequencing-by-synthesis approach

The DNA libraries for sequencing-by-synthesis approach were constructed as previously described (*S13*), with the omission of any DNA shearing step. We did not carry out any size selection steps either, as suggested by the Roche GS FLX library preparation protocol for modern DNA. DNA fragments from each sample were then blunt-ended and phosphorylated by enzymatic polishing using T4 DNA polymerase, T4 polynucleotide kinase, and *Klenow* DNA polymerase. The polished DNA fragments were then subjected to adapter ligation followed by isolation of the single-stranded template DNA (sstDNA). The quality and quantity of the sstDNA library was assessed using the Agilent 2100 Bioanalyzer. The sstDNA library fragment was captured onto a single DNA capture bead and clonally amplified within individual emulsion droplets. The emulsions were disrupted using isopropanol, the beads without an amplified sstDNA fragment were removed, and the beads with an amplified sstDNA fragment were recovered for sequencing. The recovered sstDNA beads were packed onto a 70x75mm PicoTiterPlate^{TM} at a density of 1.9 million beads per plate. In contrast to a previous study on mammoth DNA (*S3*) a sequencing system, the GS FLX (Roche Applied Science, Indianapolis, IN, U.S.A.) was used, which can generate sequencing reads of up to 250 bp. The mammoth mitochondrial genomes analyzed in this study have been deposited in **GenBank** and can be accessed under ID 0.00000000.

Data Assembly

Sequence reads aligning to the mitochondrial sequence of Krause *et al.* (*S14*) were filtered and trimmed to require at least 95% identity, then assembled using scripts to run

existing assembly software. The sequence coverage at each position within each complete mitochondrial sequences varied from 7.3- to 48.0-fold coverage (see for example Supplemental Figure 1).

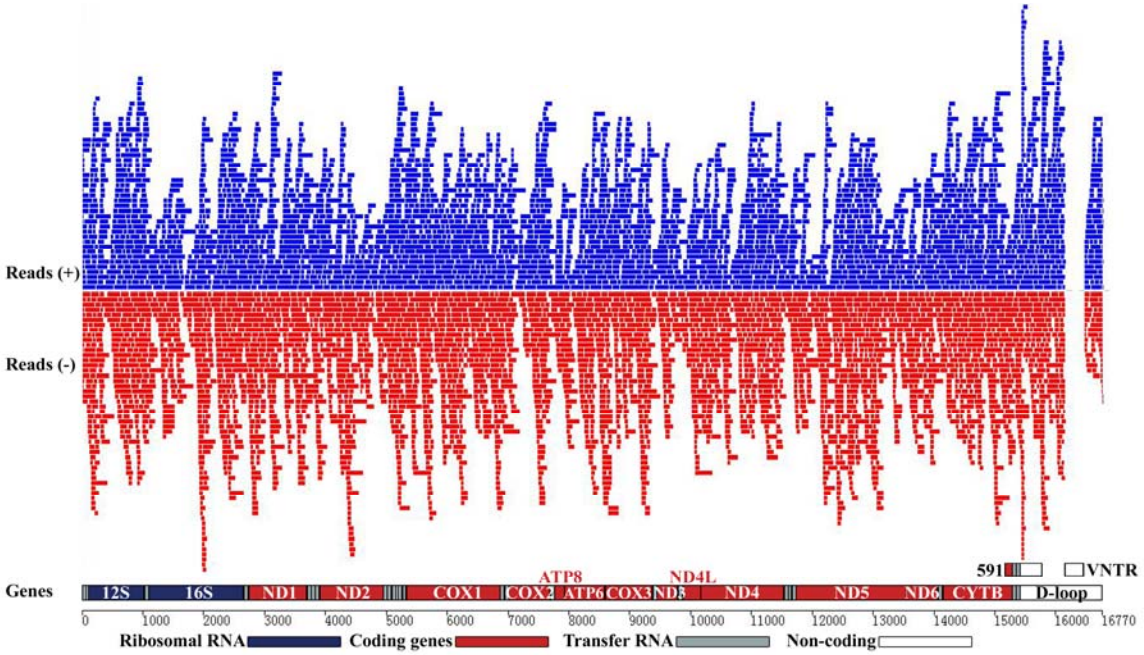

Figure S1. Assembly overview of M1 mitochondrial sequence. Blue lines indicate matches in the forward direction, while red lines depict positions of reads that had to be reverse complemented before aligning to mitochondrial genome of M1.

Sequence reconfirmation using conventional PCR and Sanger Sequencing

Conventional PCR coupled with Sanger sequencing was used to confirm and investigate the reliability of the sequencing-by-synthesis sequences generated through resequencing of the nucleotide positions that the 454 sequencing identified as divergent from the Krause (*S14*) mammoth (as discussed in the main text) on DNA extracted from M1. Details of the primers and regions amplified are in Supplemental Table 2. PCR was performed for 40 cycles using High Fidelity Platinum Taq (Invitrogen) at Penn State University, in 25µl reactions following the manufacturer's guidelines. In total 20kb of the mitochondria was sequenced. The data shows 100% agreement with 454 reads with the exception of 3 mixed alleles in the PCR. In each of these cases 1 of the 2 alleles agreed with the 454 sequence data.

Supplemental Table 2. Primers and regions amplified from specimen M1

Primer Set	Forward primer 5'→3'	First base of F primer[a]	Reverse primer 5'→3'	Amplicon Size	Annealing temperature
2	AAAGGACTGGTCAATTTCGTG	295	ACCCTAGCTATCGTATGTTTAGGA	194	60
9	GCAGTAGCCTTCCTCACCTT	2786	TCAGACTTGATATTGCGAGAATAAA	289	60
11	AACCGAGCTCCATTTGATTT	3320	TTCTGGTATTTGGGGGTTACA	180	60
12	GAACCTCTTGTAACCCCCAAA	3471	TGGGATGCATGCTAGTGAAA	215	60
15	TCCCTAACTCTAATATGAAACAAAACA	4590	AGATAGGGTGATTAGAGTCGGTAA	315	60
16	CCCCTAACCCCAATAATTTCA	4918	GATTTTCGTGGGATTGAAGC	203	60
19	CTACCCTTCATGGCGGTAATA	6304	GAATTTTGGCTCATGTATGGTTT	264	60
20	TTTATCGGTGTTAATTTGACATTCTT	6582	CGTTTGTTGTTGTGAGTTCTATCA	223	60
21	CAAGCCAACTCTATAACCTTTATGC	6911	TGGACGTTTATTATATTTGTGTGGA	286	60
22	TCCACACAAATATAATAAACGTCCA	7172	AGCTCCAGAATCATTGGTGTC	171	60
26	TCACCAAACACATGCCTATCA	8608	AAAAGGCTCAGAAGAAACCTG	299	60
27	CAGGTTTCTTCTGAGCCTTTTA	8886	GCCATAGATACCGTCGGAGA	299	60
29	CATTTACTGATGAGGATCCTATTTCTT	9367	GCGATTTCTAGGTCAAATAGGAGA	299	60
30	TTTACCCTGAGCTATCCAAGC	9678	ATTGAGGGATAATAGTGCATTTAAG	346	60
31	TGTTTACCTTAAATGCACTATTATCC	9992	GGCTAGTTAGACTAATTGCGAAGC	287	60
33	GGATCTCTCCCCCTACTAGTAACC	10629	AAGGCTATGTGGCTGACTGAA	422	60
35	TTTACCCGAGAGAACACCTTG	11451	GAAAGCCACATTGTTAGATGAGG	216	60
38	ACCCTCATCCGCTTTTATCC	12514	GCTGTTGAAGTAATGGGTATTGTTT	341	60
41	CCAAAACTCCCTTCACCAAG	13675	GGGGGATCTTTCTTGGGTCT	260	60
42	CCACTATCATCCCACCGAAA	13877	TGGTAGGAGTCCATGTAGAGGT	220	60
43	GACTAATGATCTGAAAAACCATCG	14097	TGCTCCGTTTGAGTGTAGTTG	315	60
44	CCTACCTATACTCGGAAACCTGAA	14467	AGCCTGTTTCGTGAAGGAAG	297	60
45	ACCTTCCTTCACGAAACAGG	14742	ATCGTAGGATGGCGTAAGCA	256	60
47	GGTATTCAGGGAAGAGGTCCA	15349	CACGAATATGACTTGACACATTGA	255	60
49	CCATCTTCGTGTCCCTCTTC	15784	ACCAAATGCATGACACCACA	200	60

[a]Numbering with reference to the revised Krause sequence (*S14*) GENBANK Accession DQ188829.2

Numt Analysis

Analysis of mtDNA extracted from various mammalian tissues (including hair from some elephants) is known to have complications due to the presence of so-called numts (e.g. *S15*), i.e. segments of the nuclear genome that are homologous to mitochondrial DNA, presumably as the result of a duplication/insertion event. To estimate the frequency with which numts might appear among our reads, we aligned the human, mouse, dog and African elephant mitochondrial genomes with their corresponding nuclear genome sequence, using the initial alignment thresholds being employed for the mammoth data. Human had by far the highest number of numts: 1005 in human, 328 in dog, 165 in mouse, and 176 in elephant. The respective average lengths of the numts were 446, 286, 287, and 785 bp. It is difficult to interpret the differences in these results due to the large differences in the quality of the genome assemblies, but at least the results suggest that a mammalian genome contains 50 kb to 450 kb of numts, which agrees with the data obtained for the human genome by Woischnik and Moraes (*S16*).

To obtain a crude estimate of the ratio of numt reads to mitochondrial reads in our data, suppose the mammoth nuclear genome is 3 billion bp and has 300 kb (0.01%) of numts. Assuming a random sampling of the mammoth nuclear genome, 0.01% of the mammoth nuclear sequence will be numts. Moreover, only a small fraction of the numt DNA has the potential to confound our approach, which performs a subsequent filtering step that discards any sequence having below 95% identity to the mammoth mitochondrial sequence of Krause *et al.* (*S14*). (Numts identified in a previous study on elephant hair differed from the mtDNA consensus sequence by 8-34%, *S15).* On a typical

run, roughly 1% of our reads match mtDNA, so at the very most, 1% of the matching reads (0.01% equals 1% of 1%) might be numt DNA; because of the 95%-identity restriction, the actual numt contamination is probably more like 0.1% of the putative mtDNA reads. The chances of getting at least half of the reads from numts at a position with 10x coverage can be estimated according to the binomial distribution with parameters p=0.01 and N=10; the probability of having 5 or more numts is about 2.4 x 10^{-8}. Moreover, for a miscall, the numts need to have a consensus base that differs from the correct one. The likelihood of this happening even once in the mitochondrial genome is negligible.

Mammoth hair morphology, DNA preservation in hair, and their implications for analyses on hairs from other mammalian taxa

Although we used up to 5.2g hair shaft per individual, we were able to sequence the complete mitochondrial DNA sequence from the sample that had been exposed to room temperature for the longest time (thus likely undergone the highest levels of DNA degradation), and consisted of the lowest hair weight (0.2g) (M13, the so-called 'Adams' mammoth). As such, it seems likely that the minimum amount of mammoth hair shaft that can be used in this approach is less than 0.2g. However, we acknowledge that a great deal of morphological variation exists both between specific hair types of different species, and among hairs on any particular individual (i.e. overcoat, undercoat, juvenile hair, eyelash etc). This variability, the result of subtle differences in hair biogenesis must inevitably have both effects on the DNA levels within the hair and implications for long-term DNA survival (although this has not been investigated in detail).

Factors that vary among mammals, and thus may be important include the following: The diameter of the hair fibre, the proportional composition of the three main morphological components, the cuticle (thin external layer of cells), cortex (medial layers that form the majority of the shaft) and medulla (central core section, which may or may not be present, species and hair type dependent).

The number of cuticle cells on the external surface of the hair shaft can be highly variable. For example, although the cuticle of human hair is generally between 6 and 10 cell layers thick, in wool the cuticle is only 1 cell layer thick. Furthermore, where the medulla is present there is potential for increased access by destructive microbial and chemical agents and contaminants into the fibre core. Lastly, among different hair types (both within and between species), the physical strength of the cuticle-cortex and cortex-medulla junctions may vary, which will have implications on both how quickly a hair might degrade, plus resistance to contaminant DNA. However, in regard to mammoth coat hair, high resolution light microscopy indicates that the cuticle and medulla may be either present or absent (see Supplemental Figure 2 A-D), and as such the relative contribution of the cuticle and medulla may be irrelevant.

Despite these differences however, the underlying chemical structure of hair shafts, and their fundamental biogenesis is similar between hair types. The predominant mass of the hair shaft is the cortex, comprised of cortical keratinocytes that, when fully developed (keratinized), contain numerous 7-8 nm thick intermediate hard keratin filaments that orient in the hair growth direction (*S17*). These are distributed within a matrix of non-filamentous sulphur-rich keratin-associated proteins to form macrofibrils (each roughly 300 nm in diameter) within the overlapping and interdigitating spindle-

shaped cortical cells that comprise the hair cortex. Keratinization itself is an exceedingly rapid process in hair shafts, in humans taking only 2.5 days taken from "birth" of the hair fibre cell (in contrast with the up-to-10 days required for keratinocytes in the skin) (*S18*). Although we do not know the exact rate of mammoth hair growth, stable light isotope data from Iacumin *et al.* (*S19*) shows periodicity in mammoth hair growth that suggests seasonal change in diet, which roughly equates with the growth of human scalp hair i.e. roughly 12 cm per annum.

During hair formation, as the cells undergo the terminal differentiation that culminates in the filling of the cell cytoplasm with keratin, the cells undergo organelle destruction and overall dehydration/ desiccation. This desiccation may explain the relatively low levels of hydrolytic DNA damage that this, and previous (e.g. *S4*) studies on ancient hair DNA observe. Although the organelles undergo destruction, nuclear and mitochondrial remnants are clearly visible among macrofibrils in many keratinized hair cortex cell (see Supplemental Figure 2E, also see *S4*). It seems plausible therefore that these are the sites of DNA survival, protected from both water, other potential degradative agents and exogenous sources of contamination.

DNA has been recovered and sequenced by conventional (i.e. specific-primer based PCR) from hair shafts sampled from representative species of several mammalian order, including Artiodactyls, Perissodactyls, Primates, Proboscidea and Carnivora (c.f. *S4, S15, S20, S21*, this study) thus its presence in almost all modern hairs seems likely. As the mechanistic limitation of the sequencing-by-synthesis approach adopted in this study is solely DNA quantity, no reason is obvious why our findings of the applicability of our results cannot be extended across most other mammalian taxa.

Supplemental Figure 2A-E: Well preserved terminal coat hair shaft from two separate mammoth finds as evidenced in light micrograph whole mounts and in high resolution light micrograph transverse sections stained with toluidine blue in borax.

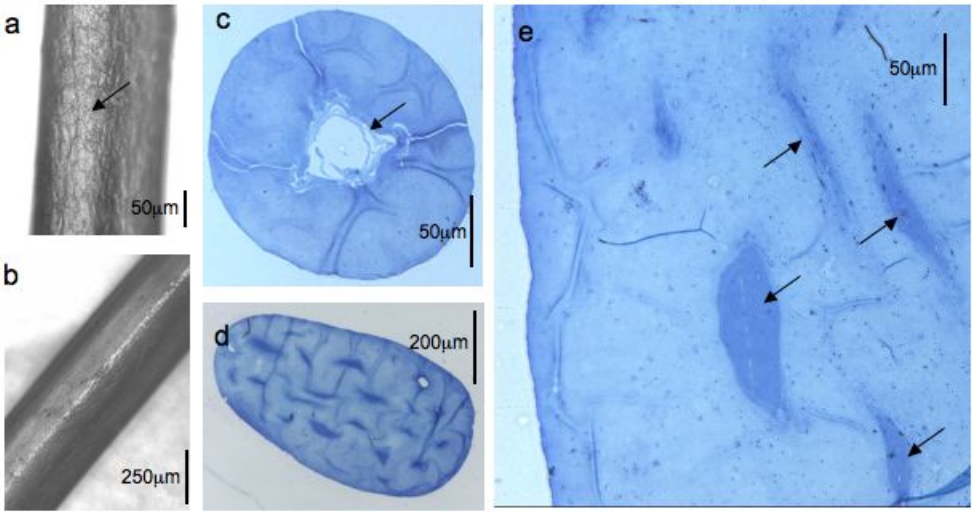

(A) Hair shaft with cuticle (arrow). (B) Hair shaft without cuticle. (C) Transverse section showing medullated shaft (arrow). (D) Transverse section showing absence of medulla and cellular differentiation with dark stained regions within the cortex also detailed in (E), which represent cellular debris destined to become 'nuclear remnants'(arrows) as the keratinized shaft is squeezed out from the skin; the small dark flecks are the mature pigment granules responsible for shaft color .

Sample thermal ages

Post mortem, the degradation of DNA correlates with both time and temperature. The so-called thermal age (defined as the time taken to produce a given degree of DNA degradation when temperature is held at a constant 10°C) has therefore been proposed as a tool to enable direct comparison between samples that differ both in age and in the temperatures they have been exposed to since death (*S22*,*S23)*. A crude calculation of the thermal age for those specimens where sufficient information for the calculation was known or could be estimated was performed following (*S23*). The samples analysed were M2 (Jarkov), M3 (Fishhook), M8 (Dima), M13 (Adams), M18, M22, M26, plus for comparison the frozen bone sample used for the generation of the Poinar mammoth sequence (*S3*). The model incorporated temperature data from weather stations local to the respective sites, with altitude correction (lapse rate of + 6.5°C km^{-1}) using elevations estimated from the sample coordinates (using GoogleEarth v.4.1). Furthermore, to control for differences in sample burial depth (and thus temperature of the burial site), the model incorporated two depths of burial for each sample, 'shallow' (where the sample temperature could be expected to fluctuate during the year) and 'deep', where the sample would experience a constant temperature, and factored in time and temperature (at a conservative assumption of 10°C) since collection. Although the calculated thermal ages will necessarily be crude due to the errors associated with the estimated parameters, it can be expected that the true thermal ages will fall between the values predicted by the extremes suggested by the two alternative models. The data indicates that the thermal age of the samples is very low, reflecting the low temperatures that the samples have been

maintained at since death (main article Figure 2). As such, the survival of amplifiable DNA is not surprising. The data indicates that of the hair samples, Dima (M8) and Adams (M13) have the highest thermal ages. The high thermal age of Dima is not surprising considering its relatively southern geographic origin, and is further exacerbated by the fact that, in contrast to the other samples, Dima has been kept at room temperature for most of the time since its recovery in 1977. The thermal age of M13 can be explained by the >200 years that the sample has spent at room temperature since initial collection. Despite these high thermal ages however, the levels of observable DNA damage within both the Adams and Dima samples are lower than in the thermally younger bone sample of Poinar *et al.* (*S3*) (main text, Table 1), that was excavated directly from permafrost and maintained frozen for its curation history. This observation provides evidence that in comparison to bone, DNA degradation rates post mortem in hair shaft are lower than anticipated.

Accelerator Mass Spectrometry (AMS)

Hair samples from mammoths M4, M8 (Dima) M18, M22 and M26 were submitted for ^{14}C dating at the Oxford Radiocarbon Accelerator Unit (ORAU), University of Oxford. Radiocarbon determinations obtained from the ORAU are shown in Table 1 (main article). The Oxford AMS radiocarbon method and instrumentation is reported by Bronk Ramsey *et al.* (*S24*).

Supplement References

S1. R.K. Thomas *et al.* Nat *Med*. **12**, 852-855 (2006).

S2. J. Binladen *et al.* PLoS ONE **2**, e197 (2007).

S3. H. N. Poinar *et al. Science* **311**, 392-394 (2006).

S4. M. T. P. Gilbert *et al. Curr. Biol.* **14**, R463-464 (2004).

S5. M. Stiller *et al. Proc. Natl. Acad. Sci. U. S. A.* **103**, 13578-13584 (2006).

S6. E. D. Robin, R. Wong R. *J. Cell. Physiol.* **136**, 507-513 (1988).

S7. E. I. Rogaev *et al. PLoS Biology* **4**, e73 (2006).

S8. M. T. P. Gilbert *et al. Curr. Biol.* **14**, R463-464 (2004).

S9. M. T. P. Gilbert *et al. Forensic Sci. Int.* **156**, 208-212 (2006).

S10. D. *Mol et al. The World of Elephants – International Congress, Rome*, pp.305-309 (2001).

S11. D. *Mol et al. The World of Elephants – International Congress, Rome*, pp.310-313 (2001).

S12. A. Heintz, W. E. Garrut. *Trans. (Dokl.) USSR Acad. Sci*. **154**, 1367-1370 (1964).

S13. M. Margulies *et al. Nature* **437**, 376-380 (2005).

S14. Krause *et al. Nature* **439**, 724-727 (2006).

S15. A. D. Greenwood, S. Pääbo. *Mol. Ecol*. **8**, 133-137 (1999).

S16. M. Woischnik, C. T. Moraes. *Genome Res*. **12**, 885-893

S17. L. Langbein, M. A. Rogers, H. Winter, S. Praetzel, J. Schweizer. *J. Biol. Chem.* **276**, 35123-32 (2001).

S18. B. Forsland, G. Swanbeck G. *Exp. Cell Res.* **43**, 191-209 (1966).

S19. P. Iacumin, S. Davanzo, V. Nikolaev. *Palaeogeogr. Palaeocl.* **218**, 317-324 (2005).

S20. R. Bonnichsen *et al. J. Archeol. Sci.* **28**, 775-785 (2001).

S21. S.I. Nakaki *et al. Forensic Sci. Int.* (in press)

S22. C. I. Smith *et al. Nature* **410**, 772-773 (2001).

S23. C.I. Smith, A.T. Chamberlain, M.S. Riley, C. Stringer, M.J. Collins. *J. Hum. Evol.* **45**, 203-217 (2003).

S24. C. Bronk Ramsey, T. F. G. Higham, P. Leach P, *Radiocarbon* **46**, 17-24 (2004).